JOURNAL OF THERMOPHYSICS AND HEAT TRANSFER
Vol. 10, No. 1, January–March 1996

Measurements of Radiative Properties of Cellular Ceramics at High Temperatures

R. Mital,* J. P. Gore,† and R. Viskanta‡
Purdue University, West Lafayette, Indiana 47907-1288

The extinction coefficient and the single scattering albedo of selected cellular (reticulated) ceramics that are candidates for use in radiant burners were determined in the 1200–1400 K temperature range. Total radiation intensities leaving layers of the reticulated material heated to steady state in a tube furnace with two different boundary conditions were measured. An inverse radiation approach involving the two-flux approximation using a gray, isotropically scattering model was used to obtain the radiative properties from the measured intensities. Above an optical thickness of unity, this procedure was not sufficiently sensitive to yield the extinction coefficient. For such cases, the extinction coefficient was estimated from the geometric optics limit. The single scattering albedos varied from 0.68 to 0.88 with an uncertainty of ±7%, whereas the extinction coefficients varied from 81 to 270 m^{-1} with an uncertainty of ±11%, depending on the number of pores per centimeter and the sample material. In the range of temperature investigation the variations in the radiation properties were not significant.

Nomenclature

b = backscattering fraction
d = pore diameter, m
f = forward scattering fraction
f_v = solid volume fraction
I = intensity, W/m²-sr
L = specimen thickness, m
p = volumetric porosity
Q_a = absorption efficiency factor
Q_s = scattering efficiency factor
T = temperature, K
δ = convergence criteria
ε = emissivity
λ = wavelength, m
ρ = reflectivity
σ = Stefan–Boltzmann constant, 5.670×10^{-8} W/m²-K⁴
σ_a = absorption coefficient, m^{-1}
σ_e = extinction coefficient, $\sigma_s + \sigma_a$, m^{-1}
σ_s = scattering coefficient, m^{-1}
τ = optical thickness, $\sigma_e^* L$
Ω = solid angle, sr
ω = scattering albedo, $\sigma_s/(\sigma_s + \sigma_a)$

Subscripts
a = absorption
e = extinction
f = furnace
s = scattering

Superscripts
$+$ = forward direction
$-$ = backward direction

Received June 7, 1995; presented as Paper 95-2036 at the AIAA 30th Thermophysics Conference, San Diego, CA, June 19–22, 1995; revision received Aug. 14, 1995; accepted for publication Aug. 17, 1995.

*Graduate Student, School of Mechanical Engineering. Student Member AIAA.
†Professor, School of Mechanical Engineering. Senior Member AIAA.
‡Professor, School of Mechanical Engineering. Fellow AIAA.

Introduction

POROUS burners with premixed natural gas/air combustion have shown the potential to provide the uniform high heat flux necessary for many industrial applications.[1] Although both metal/ceramic fiber- and cellular (reticulated) ceramics-based burners/radiant heaters have exhibited superior performance compared to other conventional burners in laboratory and field applications, systematic fundamentals-based design procedures do not exist. The reason for this is a lack of understanding of processes related to the interaction between heat transfer and combustion as a function of fuel input rate, radiant surface properties, and interaction between solid/gas phase. Since radiative transfer plays an important role in such burners, a good database for radiative properties is needed for the development and use of mathematical models of combustion–heat transfer in single- and multiple-layer porous burners–heaters. Presently, volumetric radiative property data for dispersed (porous, particulate) materials are lacking and must be established empirically using experimental measurements for materials of interest. All of the present models involving a solution of the radiative transfer equation (RTE) in high-temperature ceramic foams use assumed radiative property data or perform parametric studies.

Volumetric radiative properties of dispersed media can be determined by both direct and inverse methods. Inverse methods of determining the radiative properties involve the measurement of radiation intensity emerging from a test specimen and then constructing an appropriate radiative transfer model to determine the properties.[2] Inverse methods are more difficult, but for systems at elevated temperatures it may be the only approach that is feasible.

Inverse methods have been used for the measurement of fibrous and solid ceramic materials as well as porous cellular (reticulated, foam) structures. In the following, brief summaries of the existing works are presented.

Fibrous and Solid Ceramic Materials

Methods of determining the radiative properties (extinction coefficient, backscattering fraction, single scattering albedo, and index of refraction) of absorbing, emitting, and scattering porous fibrous materials used as high-temperature insulators have been reported.[3–6] Makino et al.[7] measured spectral reflectances of alumina, zirconia, and silicon carbide at wavelengths between 0.4–33.3 μm in the temperature range of 290–700 K. The temperature dependence of radiation prop-

erties was found to be negligible. Saboonchi et al.[8] made reflectance and transmittance measurements on fiberglass and foam insulations. For large optical thickness the albedo was determined from the reflectance measurement and the transmittance was used to determine σ_e.

Cellular Ceramics

Hsu and Howell[9] measured the extinction coefficient of highly porous (porosity greater than 80%), partially stabilized zirconia (PSZ) at high temperatures ($300 < T < 800$ K). The scattering intensity distribution was assumed to approach isotropic, and scattering albedo was not determined in this work. The extinction coefficients varied between 200 m^{-1} for 4 nominal pores per centimeter (PPC) to 1500 m^{-1} for 25 PPC. The extinction coefficient was found to decrease with increasing pore size, and, for pore size greater than 0.6 mm, the trend agreed well with the geometrical optics limit prediction.[10]

Hendricks and Howell[11] measured spectral hemispherical reflectance and transmittance in reticulated porous ceramics at room temperatures. These data were used in conjunction with the inverse analysis and a discrete ordinates model to obtain absorption and scattering coefficient and phase function. Spectral scattering albedos of PS ZrO_2 were discovered to be in the range 0.87–0.99, while those for OB SiC were lower in the range 0.55–0.88. The results also agreed with the geometrical optics theory with a slight modification to the equation used by Hsu and Howell.[9]

Peters et al.[12] suggest the use of measured spectral emission data to obtain the single scattering albedo and the transmission data to obtain the extinction coefficient for determining the radiation properties of PSZ and SiC foams. Spectral transmission, absorption, and scattering measurements have been reported. However, the data were not reduced to give values of the albedo or extinction coefficient for the porous ceramic materials. The analysis by Peters et al.[12] indicated that small optical thicknesses ($\approx \tau_L < 1$) of ceramic foam would be desirable for optimization of the radiative heat transfer rate in radiant burners.

McCarthy[13] performed three different experiments and developed analytical and physical models to determine values for the albedo, extinction coefficient, and single scattering phase function for partially stabilized zirconia (PSZ) and silicon carbide (SiC). Spectral transmittance data were obtained for different material configurations that demonstrated no spectral dependence in the region from 2.51 to 14.14 μm where data were taken. An extinction coefficient of 214 m^{-1} for 4 PPC SiC was obtained. Both materials showed little temperature dependence and exhibited a fairly gray normal spectral emissivity. The values of emissivity for SiC concentrated between 0.8–0.95 in the wavelength range of 2.5–7.5 μm. These data were used to calculate an albedo of 0.55 for SiC at 4 μm.

The specific objective of the present work was to determine extinction coefficient and single scattering albedo for cellular ceramics at high temperatures using an inverse method. The properties were determined in the 1200–1400 K temperature range since this is the expected operating range of the porous burners. Radiation properties of five materials, YZA, mullite and SiC from Selee Corporation, and cordierite and cordierite LS-2 from Hi-Tech Ceramics, Inc., are reported.

Experimental Methods

The steady-state method involved inserting the cellular ceramic samples of different thicknesses in an isothermal tube furnace. The narrow angle radiation intensities leaving the sample surface for two different boundary conditions were measured. Two equations involving extinction coefficient and single scattering albedo were obtained that were derived using an isotropic two-flux approximation to the equation of radiative transfer. The radiative properties were then recovered using the inverse method. For samples with optical thickness greater than unity ($\tau_L > 1$) the porous ceramic was approximated to be a monodispersed assembly of equivalent particles and geometrical optics limit equations were used to predict the extinction coefficients. Results of uncertainty analysis and sensitivity of parameters inherent in the model are also discussed.

Experimental Apparatus

A three-zone Lindberg furnace (type 54357-V) with an operating range of 200–1200°C was used to provide the high-temperature environment. Radiation intensity emerging in the forward direction at the boundary of the ceramic was measured using a slide mechanism,[14] a radiometer (Medtherm Corp., Huntsville, Alabama), and a sight tube (Fig. 1). The sight tube was used to prevent the radiation emitted or reflected from the cavity walls to reach the detector and the sample surface, hence, only transmission and emission of radiation by the specimen was detected. The inside wall of the sight tube was painted black to reduce internal reflection. An aluminum sight tube was chosen due to its high thermal capacity. The sight tube was cold so that it was nearly non-emitting, and from an analysis of the transient temperature response of the sight tube, it was predicted that the tube temperature would be less than 100°C if the tube remained in a 1200°C environment for half a minute. The data acquisition period was, however, less than 20 s to avoid interference from the sight tube.

The radiometer output was in mV. It was multiplied by the calibration constant of the radiometer to obtain the heat flux in W/m^2. The appropriate intensity reading was then obtained from the calibration of the sight tube. The sight tube was placed in front of the Mikron model M300 (Mikron Instrument Co., Inc., Wyckoff, New Jersey) blackbody at a known temperature and the radiometer output was recorded. The calibration constant was determined by taking a ratio of the measured flux and the Planck's blackbody radiation intensity $\sigma T^4/\pi$. All of the heat flux measurements were divided by this calibration constant to obtain the true total intensity in W/m^2sr.

Measurement Method

The specimen was placed in the center of a three-zone tube furnace (Fig. 1) and the furnace temperature was adjusted to the desired setting. When the ceramic reached a steady-state condition so that there was a single characteristic temperature for the radiating test specimen, the sight tube was quickly inserted. With the radiometer placed at the other end of the sight tube, 5000 measurements of intensity leaving the surface of the ceramic in a span of 10 s were collected using an amplifier, A/D converter, and a laboratory computer.

The intensities were measured for two boundary conditions (Fig. 2) for the specimen since two radiative properties, extinction coefficient and scattering albedo, were to be determined. In one case, a cold, highly reflective material was

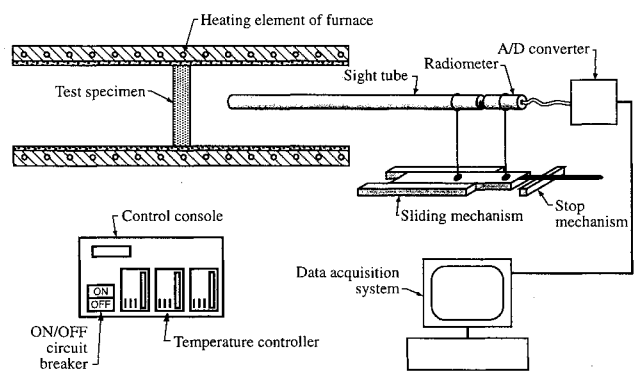

Fig. 1 Schematic of experimental setup.

Table 1 Emerging radiation intensity for the 4 PPC (10 PPI), 6.25-mm-thick YZA sample

Temperature, K	Intensity with reflector, W/m²-sr	Intensity with blackbody, W/m²-sr
1,200	22,992	24,783
1,300	30,874	34,616
1,400	38,971	46,389

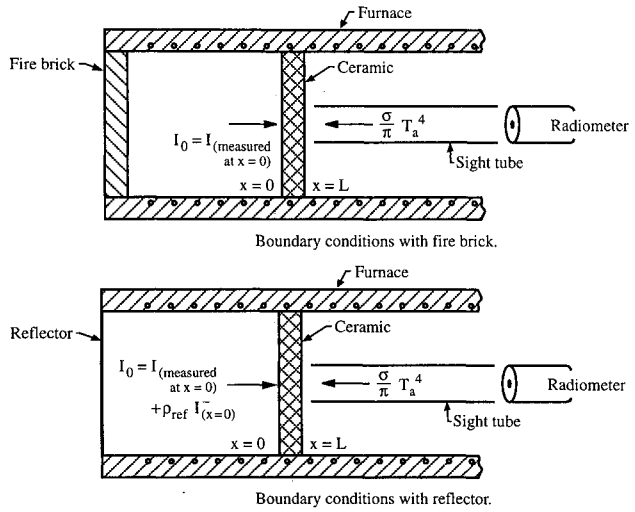

Fig. 2 Boundary conditions for the two-flux model (ρ_{ref} = reflectivity of platinum and T_a = ambient temperature).

placed at the back opening of the furnace, and in the other case the opening was closed using a firebrick, thereby simulating a blackbody environment. A platinum-coated silicon wafer was chosen as the reflector since platinum is highly reflective.[15] Only the forward-emerging intensity measurements at different temperatures were made. Sample results of these experiments for 4 PPC [10 pores per inch (PPI)], 6.25 mm thick, YZA ceramic foam are given in Table 1.

Cellular Ceramics

The cellular ceramic specimens used in the present work have been identified as candidates for use in porous radiant burners and were obtained from Selee Corporation (Hendersonville, North Carolina) and Hi-Tech Ceramics, Inc. (Alfred, New York). The specimen materials were YZA (which is approximately 35% alumina and 65% zirconia by weight), mullite, and SiC supplied by the Selee Corporation. They were of variable thicknesses, disk shaped, their porosity varied from 0.81 to 0.88, and the pore sizes were 4, 6, and 8 PPC (10, 15, and 20 PPI, respectively). Hi-Tech Ceramics, Inc., supplied cordierite and cordierite LS-2 (silicon carbide base-coated cordierite) with porosity varying from 0.7 to 0.81 and pore sizes 4, 6, and 8 PPC.

The lowest sample thickness considered was 6.25 mm, since below this thickness the homogeneous and continuum model assumption for the RTE may be violated.

Numerical Solution of the Model

The two-flux approximation was used to solve the inverse radiative transfer problem. Under this approximation, the medium is assumed to be one-dimensional and plane-parallel. More accurate methods such as S_6 discrete ordinates and others may be used, but they introduce additional unknown parameters like the phase function and, hence, were not attempted in the present work. The two-flux equations are[16]

$$\frac{dI^+}{dt} = -2(1 - f\omega)I^+ + 2\omega bI^- + 2n^2(1 - \omega)\sigma T_f^4/\pi \quad (1)$$

$$\frac{dI^-}{dt} = 2(1 - f\omega)I^- - 2\omega bI^+ - 2n^2(1 - \omega)\sigma T_f^4/\pi \quad (2)$$

where I^+ is the radiation intensity within the specimen in the direction of the detector and I^- is the radiation intensity within the specimen in the direction opposite to the detector. In the past, the two-flux approximation has been successfully used in analytical predictions for the transmittance of a packed bed of steel spheres.[10] The advantages of this model are its simplicity, relatively low computational time, and accuracy of the results, particularly for small values of optical thickness.[16] These equations are being used in most of the existing radiant burner models, hence, the resulting properties will be consistent with these codes. However, caution must be applied when using these properties with other solution methods since this may result in additional uncertainty. This is also true of the more precise methods of solution of the radiative transfer equation.

The incident intensities at the boundary of the ceramic ($x = 0$) were measured in situ without the ceramic tile in the furnace (Fig. 2). These are given in Table 2 for the reflector and the blackbody boundary conditions at different temperatures. The other inputs required for the model are the reflectivity of platinum, the backscattering fraction, and the thickness of the sample. The reflectivity of platinum was taken as 0.9[15] and the backscattering fraction was taken as 0.5, assuming isotropic scattering. This is a reasonable assumption for the present ceramic samples, based on geometric optics theory, neglecting diffraction.[12] The sensitivity of extinction coefficient and scattering albedo to inputs parameters was obtained using the numerical optimization procedure by varying one parameter at a time. A 20% change in the backscattering fraction from the base value of 0.5 leads to a 5% variation in the extinction coefficient and a 15% variation in the scattering albedo. A 5% change in the reflectivity of platinum results in less than 3% change in the value of the albedo and the extinction coefficient. Within the present experimental uncertainty, the effects of backscattering fraction are significant while those of platinum reflectivity are negligible. Therefore, these radiation properties are best suited for porous burner/radiant heater models with a constant backscattering fraction of 0.5.

The results of intensity vs optical thickness using the previous Schuster–Schwarzchild approximation are plotted in Fig. 3 for one operating condition. The intensity has been normalized with the blackbody background incident intensity I_0 given in Table 2. For the boundary condition with the blackbody background (firebrick at the back) I_0 at the back face was large and within 13% of the ideal blackbody value (Table 2). The intensity attenuated faster than the contribution due to emission from the medium. Hence, the intensities decrease with increasing optical thickness. With the cold reflector at the back face, incident intensity at ($x = 0$) was small and the emission contribution from the sample increased the intensity with increasing optical thickness. Finally, for optical thickness, $\tau_L \approx 1.5$, a balance was reached and the intensity for both the boundary conditions reached almost a constant value. Extinction coefficient of only those specimens whose optical thickness was less than unity could be determined by the present method. Since the asymptotic value of the intensity for large optical thickness is a function of the

Table 2 Boundary conditions at the back face of the ceramic ($x = 0$)

Temperature, K	Intensity with reflector, W/m²-sr	Intensity with blackbody, W/m²-sr
1,200	$\rho_{ref} I^-$ + 9,960	32,637
1,300	$\rho_{ref} I^-$ + 14,869	45,989
1,400	$\rho_{ref} I^-$ + 19,749	60,390

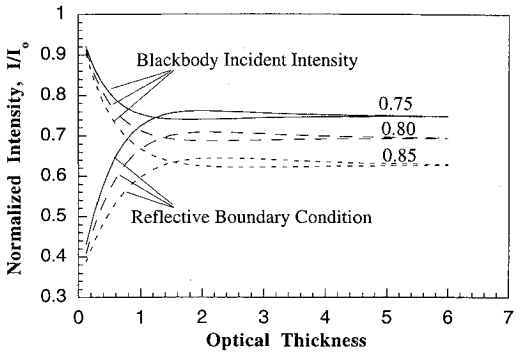

Fig. 3 Normalized intensity vs optical thickness for the two boundary conditions at 1300 K using Schuster–Schwarzchild approximation.

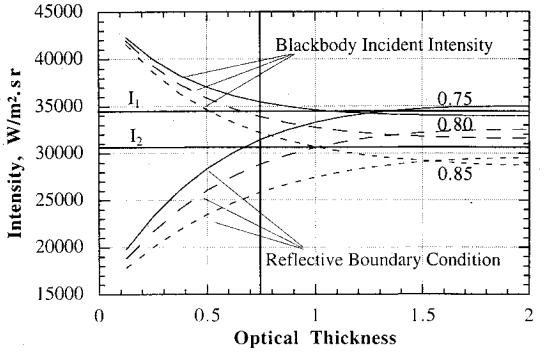

Fig. 4 Graphical determination of radiative properties for 4 PPC, 6.25-mm YZA sample at 1300 K.

single scattering albedo, this parameter can be obtained from the intensity data.

Numerical Optimization for Property Determination

The two-flux equations were written in a finite difference form and solved. In the numerical optimization procedure the unknowns (extinction coefficient and scattering albedo) were determined by applying the measurable values (the intensity for the two boundary conditions) to the theoretical analysis.

The values of scattering albedo and extinction coefficient were obtained by an iterative procedure involving matching the results of the equation of transfer and the experimental data. The procedure for 4 PPC (10 PPI), 6.25-mm samples at 1300 K is illustrated in Fig. 4. In the graphical process the experimental intensities were plotted as two horizontal lines. A value of scattering albedo was then found, the theoretical intensity curves for which intersect the two horizontal lines for the same optical thickness. This optical thickness divided by the depth of the specimen was the required value of the extinction coefficient.

In the numerical optimization procedure the equations were solved simultaneously where the value of ω and σ_e were varied until the difference between the measured intensities and the calculated intensities was less than 1%. Only the third digit accuracy of the scattering albedo was affected and the extinction coefficient changed by less than 2% by further reduction, this is shown in Table 3. In some cases an error criteria of less than 1% caused convergence problems.

Following Moffat's[17] analysis the uncertainty in the measured intensity was found to be ±7%. The numerical optimization was repeated for the worst-case scenario, one-sided biased (either +7 or −7%) errors were imposed on the intensities, and it was found that the optimized values of scattering albedo and the extinction coefficient changed by 7 and 11%, respectively. Single scattering albedo was generally observed to increase with temperature, however, since the variation in the values of the radiation properties lies within the ±7 and ±11% bounds for the scattering albedo and extinction coefficient, it was not possible to infer any trend with temperature.

Table 3 Effect of error criteria on the accuracy of the results for the 4 PPC (10 PPI), 6.25-mm-thick YZA sample

Temperature, K	Error criteria, %	Scattering albedo	Extinction coefficient, 1/m
1300	1.0	0.763	125
1300	0.66	0.764	126
1300	0.33	0.766	126

Property Determination of Samples with Optical Thickness Greater than Unity

Samples like 4 PPC (10 PPI), 12.7 mm and 6 PPC (15 PPI), 9.52 and 12.7 mm, and all thicknesses of 8 PPC (20 PPI) specimen had optical thickness greater than the resolution range of the present technique since the exit intensities (I at $x = L$) for different boundary conditions were identical within present measurement accuracy. For these samples the albedo was determined in a manner similar to that of Saboonchi et al.[8] As can be seen from Fig. 3, the intensity is a constant for optical thicknesses greater than 1.5. This constant intensity is a function of the scattering albedo. Equating the theoretical exit intensity to the experimental exit intensity for an optical thickness greater than 1.5 gave the value of scattering albedo for these samples.

The extinction coefficient can be estimated using the geometrical optics limit.[10] The porous ceramic can be represented as a monodispersed assembly of independently scattering spherical particles for large values of the parameter ($\pi d/\lambda$). For particles of d, the following relations are applicable[10]:

$$\sigma_s = (3/2)f_v(Q_s/d) = (2 - \varepsilon)(3/2d)(1 - p) \quad (3)$$

$$\sigma_a = (3/2)f_v(Q_a/d) = \varepsilon(3/2d)(1 - p) \quad (4)$$

Similar expressions have also been used by other authors[9,18,19] for radiative heat transfer calculations in porous materials. Therefore, the expression for extinction coefficient becomes

$$\sigma_e = \sigma_s + \sigma_a = (3/d)(1 - p) \quad (5)$$

The only two quantities needed to determine the extinction coefficient are the porosity and the pore diameter in meters. Both of these quantities were supplied by the manufacturer or were available in the literature. For the Selee samples porosity varied from 0.81 to 0.88 and the pore diameter was generalized by a curve fit.[20] For the Hi-Tech Ceramics, Inc. ceramic samples the porosity varied from 0.7 to 0.81 and the pore diameter was obtained from the literature[21] where a standard test method from ASTM for measuring cell size was used for Hi-Tech samples.

Results and Discussion

The results of extinction coefficient and scattering albedo for the samples with optical thicknesses less than one, which were sensitive to the present radiative property determination procedure, are presented in Table 4a–4e. The results obtained for the samples with optical thicknesses greater than one are listed in Table 5a–5e. In general, for the YZA samples (Tables 4a and 5a) the scattering albedo appears to increase with PPC. For mullite, SiC, cordierite, and cordierite LS-2 the albedo, however, appears to be independent of PPC. The scattering albedo for almost all of the samples appears to either remain constant or increase slightly with temperature.

The extinction coefficient for a fixed PPC is consistently higher for the cordierite and cordierite LS-2 samples that were

supplied by Hi-Tech Ceramics, Inc., as compared to the YZA, SiC and mullite samples that were supplied by Selee Corporation. As the PPC specification of the sample increased (i.e., the pore diameter decreased), the extinction coefficient increased (Fig. 5). The extinction coefficient did not show any specific trend with temperature for the samples considered in the range of investigation (1200–1400 K).

For the samples with optical thicknesses greater than one the albedo was numerically optimized using the exit intensities, whereas the extinction coefficient was determined using Eq. (5). To check the validity of Eq. (5), a comparison of extinction coefficients obtained using the inverse method is made with those obtained using the geometrical optics limit for the samples with optical thickness less than one (Table 6). Since Eq. (5) is not a function of temperature, mean value of the extinction coefficient given in Table 4a was used. The values obtained by the two methods are reasonably close. Hsu and Howell[9] also found that the trend for the extinction coefficient is well predicted by Eq. (5) for pore sizes larger than 0.6 mm.

According to Eq. (5), for samples of different thicknesses, but of the same PPC, a constant extinction coefficient may be expected. This is also true because the extinction coefficient and scattering albedo are material properties and should not be functions of sample thickness. However, a variation in extinction coefficient is observed in Table 5a because the porosity of the samples varies slightly due to the manufacturing tolerances from one sample to another. As much as 8% variation in porosity was observed for the samples used in the present study. The variation in radiation properties for samples with optical thickness less than one in Table 4 could be due to temperature or the uncertainty involved in the experimental measurements.

Table 4 Measurements of radiation properties for samples with optical thicknesses less than one

Temperature, K	PPC	Thickness, mm	Scattering albedo	Extinction coefficient, 1/m
		a) YZA		
1200	4.0	6.25	0.75	142
1300	4.0	6.25	0.76	125
1400	4.0	6.25	0.77	105
1300	4.0	9.52	0.81	111
1400	4.0	9.52	0.83	114
1300	6.0	6.25	0.78	129
1400	6.0	6.25	0.79	116
		b) Mullite		
1300	4.0	6.25	0.83	123
1400	4.0	6.25	0.83	131
1300	4.0	9.52	0.81	113
1400	4.0	9.52	0.81	101
1300	6.0	6.25	0.84	144
1400	6.0	6.25	0.85	142
		c) SiC		
1300	4.0	6.25	0.69	105
1400	4.0	6.25	0.71	111
1300	4.0	9.52	0.68	91
1400	4.0	9.52	0.71	98
1300	6.0	6.25	0.70	128
1400	6.0	6.25	0.70	124
		d) Cordierite		
1300	4.0	6.25	0.77	133
1400	4.0	6.25	0.77	126
1300	4.0	9.52	0.78	101
1400	4.0	9.52	0.78	97
1300	6.0	6.25	0.79	140
1400	6.0	6.25	0.78	147
		e) Cordierite LS-2		
1300	4.0	6.25	0.70	116
1400	4.0	6.25	0.70	113
1300	4.0	9.52	0.73	92
1400	4.0	9.52	0.73	93
1300	6.0	6.25	0.71	138
1400	6.0	6.25	0.71	129

Table 5 Measurements of radiation properties for samples with optical thickness greater than one

Temperature, K	PPC	Thickness, mm	Scattering albedo	Extinction coefficient, 1/m
		a) YZA		
1200	4.0	12.7	0.77	81
1300	4.0	12.7	0.83	81
1400	4.0	12.7	0.78	81
1200	6.0	9.52	0.80	178
1300	6.0	9.52	0.83	178
1200	6.0	12.7	0.80	121
1300	6.0	12.7	0.83	121
1200	8.0	6.25	0.83	188
1300	8.0	6.25	0.84	188
1200	8.0	9.52	0.83	237
1300	8.0	9.52	0.84	237
		b) Mullite		
1300	4.0	12.7	0.87	94
1400	4.0	12.7	0.88	94
1300	6.0	9.52	0.86	150
1400	6.0	9.52	0.86	150
1300	8.0	6.25	0.84	202
1400	8.0	6.25	0.85	202
		c) SiC		
1300	4.0	12.7	0.68	94
1400	4.0	12.7	0.71	94
1300	6.0	9.52	0.68	159
1400	6.0	9.52	0.71	159
1300	8.0	6.25	0.69	175
1400	8.0	6.25	0.70	175
		d) Cordierite		
1300	4.0	12.7	0.77	146
1400	4.0	12.7	0.78	146
1300	6.0	9.52	0.76	186
1400	6.0	9.52	0.77	186
1300	8.0	6.25	0.76	270
1400	8.0	6.25	0.76	270
		e) Cordierite LS-2		
1300	4.0	12.7	0.71	139
1400	4.0	12.7	0.72	139
1300	6.0	9.52	0.71	182
1400	6.0	9.52	0.71	182
1300	8.0	6.25	0.72	255
1400	8.0	6.25	0.71	255

Table 6 Comparison of extinction coefficient for ceramic samples with optical thicknesses less than one

Material	PPC	Thickness, mm	Extinction coefficient, 1/m	
			Inverse method	Geometric optics
YZA	4.0	9.52	111	94
YZA	6.0	6.25	130	158
Mullite	6.0	6.25	143	150
Cordierite	6.0	6.25	144	166

Table 7 Mean extinction coefficient and mean scattering albedo for the samples with associated standard deviation

Material	PPC	Scattering albedo	Extinction coefficient, 1/m
YZA	4.0	0.78 ± 0.03	105 ± 21.4
	6.0	0.80 ± 0.02	141 ± 24.8
	8.0	0.83 ± 0.01	212 ± 28.3
Mullite	4.0	0.84 ± 0.03	109 ± 15.5
	6.0	0.85 ± 0.01	146 ± 4.8
	8.0	0.84 ± ——	202 ± ——
SiC	4.0	0.70 ± 0.02	100 ± 7.7
	6.0	0.70 ± 0.01	142 ± 19.1
	8.0	0.69 ± ——	175 ± ——
Cordierite	4.0	0.77 ± 0.01	125 ± 21.5
	6.0	0.78 ± 0.01	165 ± 24.7
	8.0	0.76 ± ——	270 ± ——
Cordierite LS-2	4.0	0.72 ± 0.01	115 ± 20.2
	6.0	0.71 ± 0.01	158 ± 28.2
	8.0	0.72 ± ——	255 ± ——

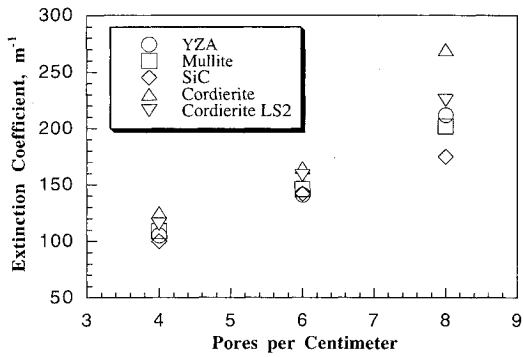

Fig. 5 Extinction coefficient vs nominal PPC for the different ceramic samples investigated.

The ensemble mean extinction coefficient and the ensemble mean scattering albedo for the different materials are listed along with the standard deviation in Table 7. Mullite has the highest scattering albedo of around 0.84 and SiC has the lowest scattering albedo of around 0.7, among all of the materials considered here. Cordierite has a relatively high scattering albedo of around 0.77. An LS-2 coating on cordierite reduces the scattering albedo to around 0.71. For a fixed extinction coefficient, a lower scattering albedo indicates a higher absorption coefficient, which is desirable for radiant burner materials.

Conclusions

The present method is suitable for the measurement of the single scattering albedos and the extinction coefficients for cellular ceramics with optical thickness less than unity. For optically thick materials, the present method yields an asymptotic value for the single scattering albedo that is used in conjunction with the geometric optics limit to obtain the extinction coefficient.

The effects of temperature on radiation properties are small within the present range.

The scattering albedo is a strong function of material and is relatively independent of PPC and temperature. The extinction coefficient is a function of both the material and the PPC of the sample. It increases monotonically with PPC. The experimental extinction coefficient correlates well with the geometric optics theory model in this study.

The present database concerning the radiation properties of cellular ceramics is useful for interactive combustion/heat transfer models of IR burners.

Acknowledgments

This work is supported by the Gas Research Institute (GRI) under Contract 5093-260-2659 with Kevin Krist serving as GRI Program Manager.

References

[1]Winter, E. M., and Brooks, D. L., "Improved Infrared Energy Transport Techniques," GRI-91/0326, Chicago, IL, March 1991.

[2]Viskanta, R., and Menguc, M. P., "Radiative Transfer in Dispersed Media," *Applied Mechanics Reviews*, Vol. 42, No. 9, 1989, pp. 241–259.

[3]Roux, J. A., Yeh, H. Y., Smith, A. M., and Wang, S. Y., "Finite Element Analysis of Radiative Transport in Fibrous Insulation," AIAA Paper 83-1502, June 1983; also *Journal of Energy*, Vol. 7, Nov.–Dec. 1983, pp. 702–709.

[4]Matthews, L. K., Viskanta, R., and Incropera, F. P., "Development of Inverse Methods for Determining Thermophysical and Radiative Properties of High-Temperature Fibrous Materials," *International Journal of Heat and Mass Transfer*, Vol. 27, No. 4, 1984, pp. 487–495.

[5]Tong, T. W., and Tien, C. L., "Analytical Model for Thermal Radiation in Fibrous Insulation," *Journal of Thermal Insulation*, Vol. 4, July 1980, pp. 27–44.

[6]Kurosaki, Y., Takeushi, M., Kashiwagi, T., and Yamada, J., "Development of Measuring Methods for Radiative Properties of Fibrous Porous Media," *Proceedings of the 1987 ASME–JSME Joint Thermal Engineering Conference*, edited by P. J. Marto and I. Tanasawa, Vol. 4, ASME–JSME, New York and Tokyo, 1987, pp. 319–325.

[7]Makino, T., Kunimoto, T., Sabai, I., and Kinoshita, H., "Thermal Radiation Properties of Ceramic Materials," *Heat Transfer Japanese Research*, Vol. 13, No. 4, 1984, pp. 33–50.

[8]Saboonchi, A., Sutton, W. H., and Love, T. J., "Direct Determination of Gray Participating Thermal Radiation Properties of Insulating Materials," *Journal of Thermophysics and Heat Transfer*, Vol. 2, No. 2, 1988, pp. 97–103.

[9]Hsu, P. F., and Howell, J. R., "Measurements of Thermal Conductivity and Optical Properties of Porous Partially Stabilized Zirconia," *Experimental Heat Transfer*, Vol. 5, No. 4, 1992, pp. 293–313.

[10]Tien, C. L., "Thermal Radiation in Packed and Fluidized Beds," *Journal of Heat Transfer*, Vol. 110, No. 4, 1988, pp. 1230–1242.

[11]Hedricks, T. J., and Howell, J. R., "Absorption/Scattering Coefficients and Scattering Phase Functions in Reticulated Porous Ceramics," *Proceedings of the AIAA/ASME 6th Thermophysics and Heat Transfer Conference*, AIAA, Washington, DC, 1994, pp. 105–113 (ASME HTD-276).

[12]Peters, J. E., Brewster, M. Q., and Buckius, R. O., "Radiative Heat Transfer Augmentation in High Temperature Combustion Systems with Application to Radiant Tube Burners," GRI-91/0101, Chicago, IL, June 1990.

[13]McCarthy, T. A., "Measurements of Infrared Radiative Transfer for Porous Ceramic Materials," M.S. Thesis, Univ. of Illinois, Urbana, IL, 1989.

[14]Vader, D. T., Viskanta, R., and Incropera, F. P., "Design and Testing of a High Temperature Emissometer for Porous and Particulate Dielectrics," *Review of Scientific Instruments*, Vol. 57, No. 1, 1986, pp. 87–93.

[15]Touloukian, Y. S., and Ho, C. Y., *Thermophysical Properties of Matter*, Vol. 7, Plenum, New York, 1972.

[16]Modest, M. F., *Radiative Heat Transfer*, McGraw-Hill, New York, 1993.

[17]Moffat, R. J., "Contribution to the Theory of Single-Sample Uncertainty Analysis," *Journal of Fluids Engineering*, Vol. 104, 1982, pp. 250–260.

[18]Kaminski, D. A., "Coupled Convection and Radiation in a Two-Layer, Porous, Volumetric Solar Collector," *Proceedings of the ASME Winter Annual Meeting*, 1990, pp. 47–53 (ASME HTD-151).

[19]Flamant, G., Menigault, T., and Schwander, D., "Combined Heat Transfer in a Semitransparent Multilayer Packed Bed," *Journal of Heat Transfer*, Vol. 110, No. 2, 1988, pp. 463–467.

[20]Haack, D., private communication, Selee Corp., Hendersonville, NC, 1993.

[21]Dam, C. Q., "Compressive Behavior and Deformation Mode Maps of Cellular Ceramics," M.S. Thesis, Pennsylvania State Univ., University Park, PA, 1988.